

# Amphiregulin triggered epidermal growth factor receptor activation confers *in vivo* crizotinib-resistance of EML4-ALK lung cancer and circumvention by epidermal growth factor receptor inhibitors

Hirokazu Taniguchi,<sup>1,2</sup> Shinji Takeuchi,<sup>1</sup> Koji Fukuda,<sup>1</sup> Takayuki Nakagawa,<sup>1,3</sup> Sachiko Arai,<sup>1</sup> Shigeki Nanjo,<sup>1</sup> Tadaaki Yamada,<sup>1</sup> Hiroyuki Yamaguchi,<sup>2</sup> Hiroshi Mukae<sup>2</sup> and Seiji Yano<sup>1</sup>

<sup>1</sup>Division of Medical Oncology, Cancer Research Institute, Kanazawa University, Kanazawa; <sup>2</sup>Department of Respiratory Medicine, Nagasaki University Graduate School of Biomedical Sciences, Nagasaki; <sup>3</sup>Tsukuba Laboratory, Eisai Co., Ltd, Tsukuba, Japan

## Key words

Amphiregulin, crizotinib-resistance, EML4-ALK, epidermal growth factor receptor, lung cancer

## Correspondence

Seiji Yano, Division of Medical Oncology, Cancer Research Institute, Kanazawa University, 13-1 Takara-machi, Kanazawa, Ishikawa 920-0934, Japan.  
Tel: +81-76-265-2794; Fax: +81-76-234-4524;  
E-mail: syano@staff.kanazawa-u.ac.jp

## Funding Information

JSPS KAKENHI (JP16H05308).

Received July 19, 2016; Revised October 17, 2016;  
Accepted October 22, 2016

Cancer Sci 108 (2017) 53–60

doi: 10.1111/cas.13111

Crizotinib, a first-generation anaplastic lymphoma kinase (ALK) tyrosine-kinase inhibitor, is known to be effective against echinoderm microtubule-associated protein-like 4 (EML4)-ALK-positive non-small cell lung cancers. Nonetheless, the tumors subsequently become resistant to crizotinib and recur in almost every case. The mechanism of the acquired resistance needs to be deciphered. In this study, we established crizotinib-resistant cells (A925LPE3-CR) via long-term administration of crizotinib to a mouse model of pleural carcinomatous effusions; this model involved implantation of the A925LPE3 cell line, which harbors the EML4-ALK gene rearrangement. The resistant cells did not have the secondary ALK mutations frequently occurring in crizotinib-resistant cells, and these cells were cross-resistant to alectinib and ceritinib as well. In cell clone #2, which is one of the clones of A925LPE3-CR, crizotinib sensitivity was restored via the inhibition of epidermal growth factor receptor (EGFR) by means of an EGFR tyrosine-kinase inhibitor (erlotinib) or an anti-EGFR antibody (cetuximab) *in vitro* and in the murine xenograft model. Cell clone #2 did not have an EGFR mutation, but the expression of amphiregulin (AREG), one of EGFR ligands, was significantly increased. A knockdown of AREG with small interfering RNAs restored the sensitivity to crizotinib. These data suggest that overexpression of EGFR ligands such as AREG can cause resistance to crizotinib, and that inhibition of EGFR signaling may be a promising strategy to overcome crizotinib resistance in EML4-ALK lung cancer.

Echinoderm microtubule-associated protein-like 4 (EML4)-anaplastic lymphoma kinase (ALK) positive lung cancer accounts for 3–5% of lung adenocarcinoma; it is more prevalent in younger people and non- or light-smokers.<sup>(1–3)</sup> Crizotinib, a first-generation ALK-tyrosine kinase inhibitor (TKI), is known to be effective against EML4-ALK-positive lung cancer. In clinical trials, the response rate has been found to be 60–74%, and progression-free survival (PFS) is 7.7–10.9 months.<sup>(4–6)</sup>

Crizotinib initially shrinks tumors, but tumors subsequently become resistant and recur in almost every case. Previous studies have described several mechanisms of resistance to crizotinib: secondary mutations of ALK (e.g. L1196M, F1174L, C1156Y, G1202R, S1206Y, and G1269A),<sup>(7–10)</sup> ALK gene amplification,<sup>(7,8,11)</sup> activation of bypass signaling (e.g. EGFR, c-KIT, IGF-1R and HER3), and activation of other driver oncogenes (mutated EGFR and KRAS).<sup>(7,10,12)</sup>

The second-generation ALK inhibitors alectinib and ceritinib have the ability to overcome resistance to crizotinib due to several secondary mutations, including L1196M, an ALK gatekeeper mutation.<sup>(13)</sup> Alectinib is reported to have a response

rate of 45% and a disease control rate of 79% in patients with EML4-ALK-positive lung cancer that is resistant to crizotinib.<sup>(14)</sup> However, resistance to second-generation ALK inhibitors has been reported to occur owing to differing ALK mutations and bypass signaling.<sup>(15–17)</sup>

Lung adenocarcinoma is often accompanied by carcinomatous pleurisy.<sup>(4)</sup> Worsening carcinomatous pleurisy is evident in many patients who display signs of resistance to targeted molecular therapy. In fact, L1196M and C1156Y (ALK mutations associated with crizotinib resistance) have been identified in malignant pleural effusions from patients with EML4-ALK-positive lung cancer that is resistant to crizotinib.<sup>(9)</sup> To ascertain the molecular mechanism for resistance to ALK inhibitors in EML4-ALK-positive lung cancer and carcinomatous pleurisy, we previously established an *in vivo* imaging model by implanting EML4-ALK-positive lung cancer cells in the thoracic cavity of animals and monitored the progression of that cancer.<sup>(18)</sup> A crizotinib-resistant cell line derived from an *in vivo* model was used in the present study, which ascertained how amphiregulin (AREG), an EGFR ligand, is largely

responsible for the activation of EGFR bypass signaling that in turn leads to resistance to crizotinib. In addition, the present study ascertained how crizotinib resistance could be overcome by inhibiting bypass signaling with EGFR inhibitors.

## Materials and Methods

**Cell cultures and reagents.** A human lung adenocarcinoma cell line, A925L, and its highly tumorigenic variant, A925LPE3, with an *EML4-ALK* fusion protein (variant 5a, E2: A20)<sup>(18)</sup> were used in this study. All cells were maintained in RPMI-1640 medium supplemented with 10% FBS, penicillin (100 U/mL), and streptomycin (10 µg/mL) in a humidified CO<sub>2</sub> incubator at 37°C. All cells were passaged for less than 3 months before renewal from frozen early-passage stocks. Cells were regularly screened for mycoplasma using a MycoAlert Mycoplasma Detection Kit (Lonza, Rockland, ME, USA). Erlotinib, alectinib and ceritinib were obtained from Selleck Chemicals (Houston, TX, USA), crizotinib was obtained from Active Biochem (Hong Kong, China), and cetuximab was obtained from Merck Serono (Darmstadt, Germany), recombinant AREG was obtained from R&D Systems.

**Antibodies and western blot analysis.** Protein aliquots of 25 µg each were separated with sodium dodecyl sulfate-polyacrylamide gel electrophoresis (SDS-PAGE) (Bio-Rad, Hercules, CA, USA) and transferred to polyvinylidene difluoride membranes (Bio-Rad). Membranes were washed three times and then incubated with Blocking One solution (Nacalai Tesque, Inc., Kyoto, Japan) for 1 h at room temperature. The membranes were incubated overnight at 4°C with primary antibodies against anti-ALK (C26G7), anti-phospho-ALK (Tyr1604), anti-phospho-EGFR (Tyr1068), anti-AKT, anti-phospho-AKT (Ser473), cleaved PARP (Asp214), anti-β-actin (13E5) antibodies (1:1000 dilution each; Cell Signaling Technology, Danvers, MA, USA), and anti-human EGFR (1 µg/mL), anti-human/mouse/rat extracellular signal-regulated kinase (Erk)1/Erk2 (0.2 µg/mL), or anti-phospho-Erk1/Erk2 (T202/Y204) (0.1 µg/mL) antibodies (R&D Systems). The membranes were washed three times and then incubated for 1 h at room temperature with species-specific horseradish peroxidase-conjugated secondary antibodies. Immunoreactive bands were visualized with SuperSignal West Dura Extended Duration Substrate, an enhanced chemiluminescent substrate (Pierce Biotechnology, Rockford, IL, USA). Each experiment was performed independently at least three times.

**Cell viability assay.** Cell viability was measured using the MTT<sup>(19)</sup> dye reduction method. Tumor cells ( $2-3 \times 10^3$  cells/100 µL/well) in RPMI 1640 medium with 10% FBS were plated onto 96-well plates and cultured with the indicated compound for 72 h. Afterwards, 50 µg of the MTT solution (2 mg/mL, 21; Sigma, St. Louis, MO, USA) was added to each well. Plates were incubated for 2 h, the medium was removed, and the dark blue crystals in each well were dissolved in 100 µL of DMSO. Absorbance was measured with a microplate reader at a test wavelength of 550 nm and a reference wavelength of 630 nm. Percent growth was determined relative to untreated controls. Experiments were repeated at least three times with triplicate samples.

**Short interfering RNA knockdown.** Duplexed Stealth RNAi (Invitrogen) against *EGFR* and *AREG*, Stealth RNAi-negative control low GC Duplex #3 (Invitrogen), and *ALK* (Dharmacon, Lafayette, CO, USA) were used for RNA interference (RNAi) assays (DOC. S1). Briefly, aliquots of  $1-2 \times 10^5$  cells in 2 mL of antibiotic-free medium were plated into each well of

a 6-well plate and incubated at 37°C for 24 h. The cells were transfected with siRNA (250 pmol) or scrambled RNA using Lipofectamine 2000 (5 µL) in accordance with the manufacturer's instructions (Invitrogen).

**Cytokine production.** Cells ( $2 \times 10^5$ ) were cultured in RPMI-1640 medium with 10% FBS for 24 h, washed with PBS, and incubated for 48 h in 2 mL of the same medium. The culture medium was harvested and centrifuged, and the supernatant was stored at -70°C until analysis. Levels of AREG, β-cellulin, transforming growth factor-α (TGF-α), HB-EGF, and EGF were determined with Quantikine enzyme-linked immunosorbent assay (ELISA) kits (R&D Systems) for those cytokines in accordance with the manufacturer's protocols. All culture supernatants were tested twice. Color intensity was measured at 450 nm using a spectrophotometric plate reader. Concentrations of growth factors were determined in comparison to standard curves.

**Tumor cell inoculation in mice with SCID.** Five-week-old male mice with severe combined immunodeficiency (SCID) were obtained from Clea Japan (Tokyo, Japan). All animal experiments complied with the Guidelines of the Institute for Laboratory Animals, Advanced Science Research Center, Kanazawa University. For the pleural carcinomatosis model,<sup>(20)</sup> an incision was made in the skin and subcutaneous tissue on the right side of the chest and the parietal pleura was exposed. A 27-G needle was then used to inject tumor cells ( $1 \times 10^6/0.1$  mL) through the parietal pleura into the right thoracic cavity. The incision was subsequently sutured closed. Tumor luminescence and mouse body weight were measured twice a week. For the subcutaneous tumor model, cultured tumor cells (A925LPE3 and #2;  $1.5 \times 10^6$  cells/0.1 mL) were subcutaneously implanted into the flanks of each mouse. The size of the subcutaneous tumors and the body weight of the mice were measured twice a week, using calipers, and tumor volume was calculated in mm<sup>3</sup> (width<sup>2</sup> × length/2). At 10 days after inoculation, mice were administered the vehicle, crizotinib, or erlotinib orally, cetuximab intraperitoneally, or a combination for 15 days. This study was carried out in strict accordance with the recommendations in the Guide for the Care and Use of Laboratory Animals of the Ministry of Education, Culture, Sports, Science, and Technology, Japan. The protocol was approved by the Ethics Committee on the Use of Laboratory Animals and the Advanced Science Research Center, Kanazawa University, Kanazawa, Japan (approval no. AP-153499). Surgery was performed once animals were anesthetized with sodium pentobarbital, and efforts were made to minimize animal suffering. According to institutional guidelines, mice were sacrificed using an overdose of sodium pentobarbital, when their tumor volume reached 1000 mm<sup>3</sup>.

**Luciferase expression and radiographic analyses with an IVIS imaging system.** After inoculation, the quantity of tumors was tracked in live mice by repeated noninvasive optical imaging of tumor-specific luciferase activity using the IVIS Lumina XR Imaging System (PerkinElmer, Alameda, CA, USA). Mice were anesthetized with 2% isoflurane and intraperitoneally injected with the luciferase substrate luciferin (150 mg/kg). Twenty minutes later, the mice were photographed under bright-field illumination and the images were overlaid with luminescence data gathered over the maximum exposure period (5–30 s). The intensity of the bioluminescence signal was analyzed with Living Image 4.0 software (PerkinElmer) by serially quantifying the peak photon flux in the selected region of interest (ROI) within the tumor. The intensity of the bioluminescence signal was corrected for the total area of the ROI

and elapsed time during which bioluminescence signals were read by the CCD camera, and this value was expressed as photons/s/cm<sup>2</sup>/sr.

**Histological analyses of tumors.** Formalin fixed, paraffin embedded tissue sections (4 μm thick) were deparaffinized. Proliferating cells were detected by incubating tissue sections with Ki-67 antibody (Clone MIB-1; DAKO Corp, Glostrup, Denmark). Antigen was retrieved by microwaving tissue sections in 10 mM citrate buffer (pH 6.0). After incubation with secondary antibody and treatment with the Vectastain ABC Kit (Vector Laboratories, Burlingame, CA, USA), peroxidase activity was visualized using the DAB reaction. The sections were counterstained with hematoxylin.

**Quantification of immunohistochemistry results.** The five areas containing the highest numbers of stained cells within each section were selected for histologic quantitation by light or fluorescent microscopy at 400-fold magnification.

**Statistical analysis.** Differences between groups were analyzed with one-way analysis of variance (ANOVA). All statistical analyses were performed using GraphPad StatMate 4 (GraphPad Software, Inc., San Diego, CA, USA).  $P < 0.05$  was considered significant.

## Results

**Crizotinib-resistant EML4-ALK-positive lung cancer cells were established in a model of carcinomatous pleurisy.** A925LPE3 cells were implanted in the thoracic cavity of mice with SCID

in order to establish a model of carcinomatous pleurisy and obtain cells that were resistant to crizotinib. A925LPE3 and A925L had similar sensitivity to crizotinib (Fig. S1). Crizotinib was administered daily (50 mg/kg) starting on day 12 after the implantation of cancer cells. Tumor luminescence gradually increased starting from day 40 after implantation. These results suggested that the cells in the thoracic cavity were crizotinib-resistant. On day 70 after the implantation of cancer cells, the mice were sacrificed. The cells were collected from the pleural effusions and cultured *in vitro* to establish the A925LPE-CR (APE-CR) cell line. They were then cloned by limiting dilution to establish the #2 cell line (Fig. 1a). APE-CR and #2 cells had different morphologies than that of A925LPE3 cells (Fig. S2a).

APE-CR cells and #2 cells, clones of APE-CR cells were resistant to the ALK inhibitor crizotinib, as well as cross-resistant to alectinib and ceritinib (Fig. 1b). Secondary ALK mutations were not detected in APE-CR cells or #2 cells (data not shown). The ALK expression was knocked down with specific siRNA in order to examine whether resistance was dependent on the ALK. The viability of A925LPE3 cells (the parent cell line) was inhibited by si-ALK, but the viability of APE-CR cells and #2 cells was not inhibited (Fig. 1c), indicating that the latter two cell lines have the resistance mechanism independent of ALK. While epithelial to mesenchymal transition (EMT) is thought to be an important mechanism of resistance against various types of kinase inhibitors,<sup>(21,22)</sup> #2 cells did not show a typical mesenchymal phenotype (Fig. S2b). Thus,

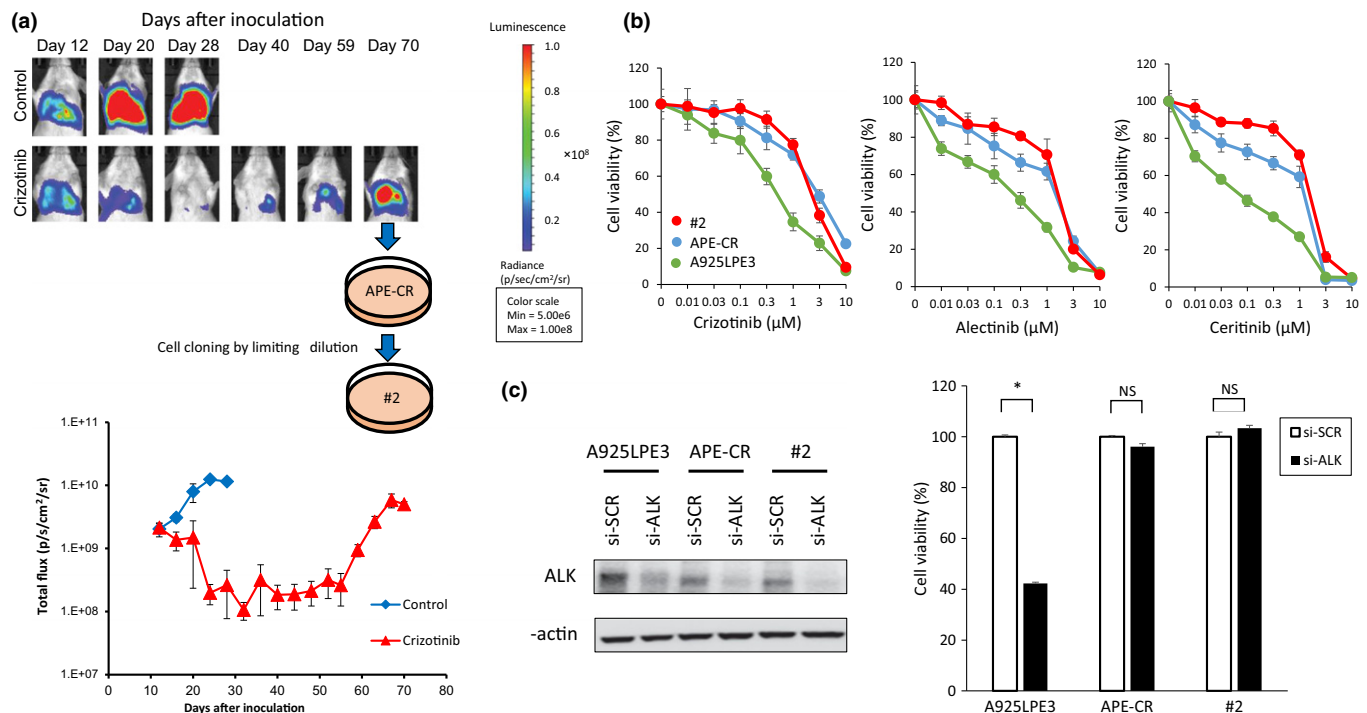


**Fig 1.** Establishment of APE-CR and #2 cell lines. (a) A925LPE3 cells were inoculated into the thoracic cavity of SCID mice. Mice were treated with crizotinib 50 mg/kg. Treatment was given daily on days 12–70. (upper). Cancer cells were collected from pleural effusions and cultured *in vitro* to establish the A925LPE-CR (APE-CR) cell line. Those cells were cloned via limiting dilution to also establish the #2 cell line. Luminescence was evaluated twice per week. Mean  $\pm$  SE of total flux are shown. (photons/s/cm<sup>2</sup>/sr). (b) APE-CR and #2 cell lines were resistant for crizotinib. A925LPE3, APE-CR, and #2 cells ( $2 \times 10^3$  per well) were incubated with various concentrations of crizotinib, alectinib or ceritinib for 72 h. Cell viability was determined by MTT assay. The data shown represent the means  $\pm$  SD of three independent experiments. (c) A925LPE3, APE-CR, and #2 cells were treated with siRNAs specific for ALK (si-ALK, respectively), or scrambled controls (SCR). (Left) Cell lysates were evaluated for protein expression by western blot 48 h later. Three independent experiments were performed, and a representative result is shown. (Right) Cell viability was determined by MTT assay 72 h later. Data represents the mean  $\pm$  SD of three independent experiments. \* $P < 0.05$  by Student's *t*-test, si-SCR versus si-ALK.

crizotinib resistance in these two cell lines is hypothesized to be triggered by other driver oncogenes or by activation of bypass signaling.

**#2 cells become resistant to crizotinib as a result of EGFR bypass signaling.** Previous studies reported that crizotinib resistance can be caused by activation of various bypass signaling pathways, including such as the EGFR, c-KIT, IGF-1R.

Here, we found that erlotinib, an EGFR-TKI, and cetuximab, an anti-EGFR antibody, restored the crizotinib sensitivity of #2 cells, but erlotinib and cetuximab individually had little effect on A925LPE3 cells (Fig. 2a,c). Neither erlotinib nor cetuximab sufficiently restored the crizotinib sensitivity of APE-CR cells (Fig. S3). Additionally, in parallel experiments, erlotinib and cetuximab restored the sensitivity of #2 cells to alectinib and ceritinib (Fig. 2b). The #2 cells were found to lack *EGFR* mutations such as an exon 19 deletion and L858R mutation (data not shown).

We next examined the protein expression and phosphorylation of EGFR, ALK, and their downstream molecules in order to determine the molecular mechanism for crizotinib resistance. When A925LPE3 cells were treated with crizotinib alone, the phosphorylation of ALK and of the downstream molecules AKT and ERK was almost completely inhibited.

When #2 cells were treated with crizotinib alone, phosphorylation of ALK was inhibited almost completely. While crizotinib inhibited the phosphorylation of AKT and ERK, the inhibition was not complete. Importantly, the combined use of erlotinib or cetuximab inhibited the phosphorylation of EGFR and thereby inhibited phosphorylation of AKT and ERK almost completely (Fig. 2c). We also examined the expression of cleaved PARP by western blotting to assess apoptosis. The combined use of crizotinib and erlotinib or cetuximab led to higher expression of cleaved PARP than crizotinib alone (Fig. S4).

We next knocked down *EGFR* with specific siRNA in order to examine whether re-sensitization of #2 cells to crizotinib by erlotinib or cetuximab was mediated by EGFR inhibition. Knocking down EGFR with siRNA restored the crizotinib sensitivity of the #2 cells. Moreover, phosphorylation of AKT and ERK was markedly inhibited by the knockdown of EGFR in the presence of crizotinib (Fig. 2d).

These findings indicate that bypass signaling via EGFR is primarily responsible for the crizotinib resistance of #2 cells.

**#2 cells expressed high levels of AREG and had activated EGFR.** Because the #2 cells did not have *EGFR* mutations, the mechanism of activation of EGFR bypass signaling was presumed to

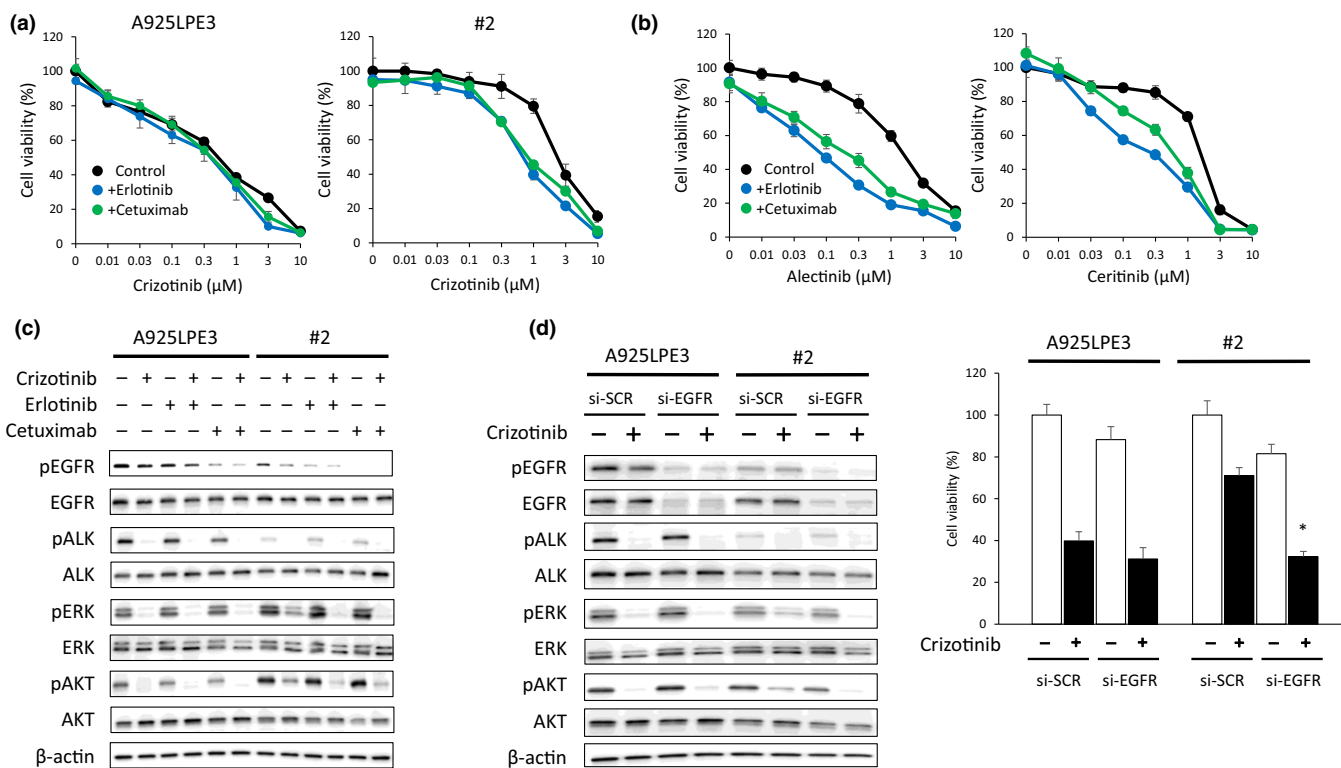


**Fig 2.** The effect of combination therapy ALK-TKI and EGFR-TKI or anti-EGFR antibody. (a) A925LPE3 and #2 cells ( $2 \times 10^3$  per well) were incubated with various concentrations of crizotinib with or without erlotinib (1 μM) or cetuximab (50 μg/mL) for 72 h. Cell viability was determined by MTT assay. The data shown represent the means  $\pm$  SD of three independent experiments. (b) #2 cells ( $2 \times 10^3$  per well) were incubated with various concentrations of alectinib or ceritinib with or without erlotinib (1 μM) or cetuximab (50 μg/mL) for 72 h. Cell viability was determined by MTT assay. The data shown represent the means  $\pm$  SD of three independent experiments. (c) A925LPE3 and #2 cells were treated with crizotinib (1 μM) and/or erlotinib (1 μM) or cetuximab (50 μg/mL) for 1 h. Cell lysates were evaluated for protein expression by western blot. Three independent experiments were performed, and a representative result is shown. (d) A925LPE3 and #2 cells were treated with siRNAs specific for *EGFR* (si-EGFR, respectively), or SCR. (Left) #2 cells with or without crizotinib (1 μM) for 1 h, following transfection with siRNA. Cell lysates were evaluated for protein expression by western blot. Three independent experiments were performed, and a representative result is shown. (Right) #2 cells were treated with crizotinib (1 μM) following transfection with si-RNA. Cell viability was determined by MTT assay 72 h later. Data represents the mean  $\pm$  SD. \**P* < 0.05 by Student's *t*-test, the group treated with si-SCR and crizotinib versus the group treated with si-EGFR and crizotinib.

involve EGFR ligands. Accordingly, the levels of five EGFR ligands (AREG,  $\beta$ -cellulin, TGF- $\alpha$ , HB-EGF, and EGF) were measured in the cell culture supernatant by ELISA (Fig. 3a).

The #2 cells expressed higher levels of AREG than the A925LPE3 cells. However, #2 cells produced lower levels of other EGFR ligands than A925LPE3 cells. These findings suggest that AREG had the greatest impact on EGFR bypass signaling in #2 cells. Thus, AREG was knocked down with siRNA in #2 cells to determine whether crizotinib sensitivity could be restored. When siRNAs specific for AREG were used along with crizotinib, crizotinib sensitivity was restored. The extent to which crizotinib sensitivity was restored coincided with the extent to which the expression of AREG was inhibited (Fig. 3b,c).

Conversely, we treated A925LPE3 cells with recombinant AREG, to examine whether AREG induces resistance to crizotinib. Exogenous recombinant AREG induced the resistance of A925LPE3 cells to crizotinib (Fig. S5).

These results indicate that EGFR activation, caused predominantly by AREG, induced crizotinib resistance in #2 cells.

**Use of crizotinib and an EGFR inhibitor inhibited the growth of #2 tumor cells *in vivo*.** We sought to determine the effect of

EGFR inhibitors when combined with crizotinib against tumors produced with #2 cells *in vivo*. A925LPE3 or #2 cells were subcutaneously implanted in SCID mice in order to produce tumors. A925LPE3 tumors shrank markedly when treated with crizotinib (Figs 4a and S6b). Western blotting indicated that the phosphorylation of AKT and ERK was inhibited in A925LPE3 tumors by treatment with crizotinib (Fig. 4c). In parallel experiments with #2 cells, the mice were divided into six groups and treated as follows: vehicle (control), erlotinib alone, cetuximab alone, crizotinib alone, crizotinib + erlotinib, and crizotinib + cetuximab. Compared to the control group, mice receiving crizotinib alone had slower tumor enlargement, but the tumor did not regress, indicating that #2 cells were resistant to crizotinib *in vivo*. Tumor enlargement was not inhibited in mice receiving erlotinib or cetuximab alone, but tumor shrinkage or arrested tumor enlargement was noted in mice receiving crizotinib combined with erlotinib or cetuximab (Figs 4b and S6b). Western blotting of the treated subcutaneous tumors indicated that phosphorylation of AKT and ERK was markedly inhibited in mice receiving crizotinib combined with erlotinib or cetuximab (Fig. 4d). Immunohistochemistry revealed that the number of Ki-67-positive proliferating tumor

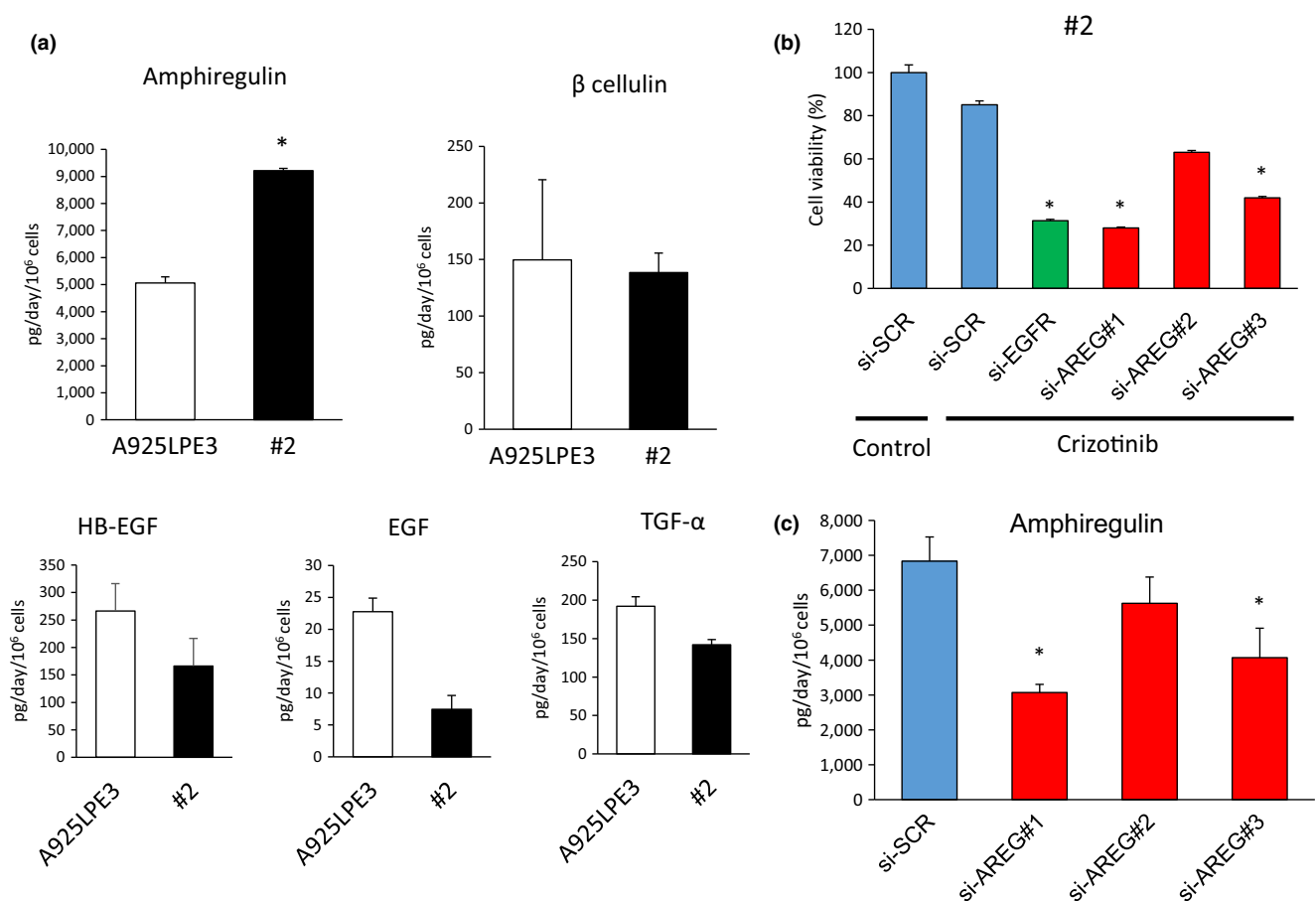


**Fig 3.** Increase of AREG caused the resistance for crizotinib. (a) Five EGFR ligands (AREG,  $\beta$  cellulin, HB-EGF, EGF, and TGF- $\alpha$ ) production by #2 cells. The cells were incubated in medium for 48 h and culture supernatants were harvested. The level of ligands in the supernatants was determined by ELISA. \* $P < 0.05$  by Student *t*-test, #2 versus A925LPE3. (b) #2 cells were treated with or without crizotinib (1  $\mu$ M) for 72 h following transfection with siRNAs for EGFR or AREG (si-EGFR and si-AREG, respectively), or SCR. Cell viability was determined by MTT assay. The data shown represent the means  $\pm$  SD of three independent experiments. \* $P < 0.05$  by Student's *t*-test, versus the group treated with si-SCR and crizotinib. (c) AREG production by #2 cells were decreased after transfection with si-AREG. The cells were incubated in medium for 48 h and culture supernatants were harvested. The level of ligand in the supernatants was determined by ELISA. Data represents the mean  $\pm$  SD. \* $P < 0.05$  by Student's *t*-test, versus the group treated with si-SCR.

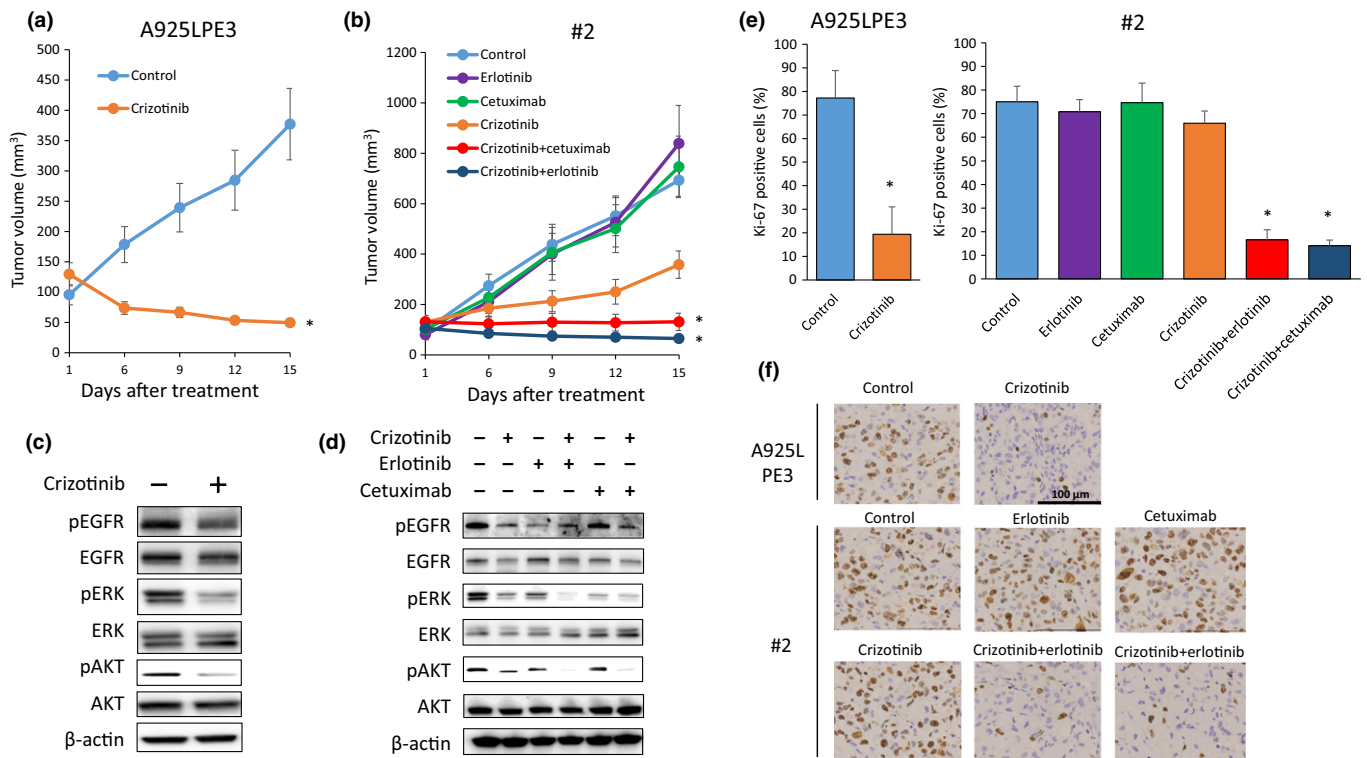


**Fig 4.** Epidermal growth factor receptor (EGFR) inhibitor combined with crizotinib overcome resistance to crizotinib *in vivo*. (a) A925LPE3 cells were inoculated subcutaneously into SCID mice ( $n = 5$ , each group). Daily oral treatment with vehicle (control) or crizotinib (50 mg/kg) was given for 15 days. Mean  $\pm$  SE tumor volumes are shown. \* $P < 0.05$  by Mann–Whitney test, versus control group. (b) #2 cells were inoculated subcutaneously into SCID mice ( $n = 5$ , each group). And the mice were randomized into vehicle (control), erlotinib (25 mg/kg), cetuximab (1 mg/twice a week), crizotinib (50 mg/kg), crizotinib (50 mg/kg) + erlotinib (25 mg/kg), and crizotinib (50 mg/kg) + cetuximab (1 mg/twice a week) treatment groups. The treatment was given for 15 days. Tumor volume was measured using calipers on the indicated days. Mean  $\pm$  SE tumor volumes are shown. \* $P < 0.05$  by Mann–Whitney test, versus the group treated with crizotinib. (c) (d) A925LPE3 or #2 tumors were resected from the mice 3 h after administration. And the relative levels of proteins in the tumor lysates were determined by western blot analysis. (e) Quantification of proliferative cells, as determined by their Ki-67-positive proliferation index (percentage of Ki-67-positive cells). The data shown represent the means of five areas  $\pm$  SD. \* $P < 0.05$  by Student's *t*-test, versus control group in A925LPE3, versus the group treated with crizotinib in #2. (f) Representative images of A925LPE3 and #2 tumors immunohistochemically stained with antibodies to human Ki-67. Bar, 100  $\mu$ m.

cells remarkably decreased in #2 cell tumors treated crizotinib combined with erlotinib or cetuximab, compared with control tumors or tumors treated with either monotherapy (Fig. 4e,f). These results indicate that the crizotinib resistance of #2 cells was overcome *in vivo* through the use of an EGFR inhibitor and crizotinib. None of the groups of mice had significant weight loss (Fig. S6a).

## Discussion

Epidermal growth factor receptor activation is known to confer crizotinib resistance to *ALK*-positive NSCLC cells.<sup>(8,10,23)</sup> However, EGFR can be activated by various ligands, including EGF, TGF- $\alpha$ , HB-EGF, and amphiregulin.<sup>(24)</sup> To the best of our knowledge, there are two reports showing the association between amphiregulin expression and crizotinib resistance via EGFR activation.<sup>(8,10)</sup> In these two reports, the involvement of AREG on crizotinib resistance was not directly verified, but circumvention of crizotinib resistance by EGFR inhibitors or EGFR knockdown was clearly demonstrated. The present study reports three novel findings. First, using *AREG*-specific siRNA, we clearly demonstrated the involvement of AREG in the acquisition of crizotinib resistance. Second, we demonstrated that AREG-triggered crizotinib resistance could be induced in NSCLC cells (A925LPE3) expressing the unique *EML4-ALK*

variant (E2:A20). To date, crizotinib resistance associated with AREG overexpression has been reported in NSCLC cells expressing other *EML4-ALK* variants (H3122 cells with E13:A20 and DFC1076 cells with E6:A20). Third, we demonstrated that AREG-triggered crizotinib resistance could be induced in a pleural effusion mouse model by daily oral treatment with crizotinib. To date, the association between AREG overexpression and crizotinib resistance has been demonstrated in: (i) cells that acquired crizotinib resistance through *in vitro* culture with increasing concentrations of crizotinib; and (ii) cells derived from clinical specimens of a patient who acquired crizotinib resistance. Our findings indicate that the pleural carcinomatosis mouse model with human *EML4-ALK* NSCLC cells would be an effective tool for identifying clinically relevant resistance mechanisms.

Activation of bypass signaling is a well-established resistance mechanism for targeted therapy. *EML4-ALK*-positive lung cancer is reported to develop resistance to crizotinib through bypass signaling via pathways such as c-KIT,<sup>(8)</sup> EGFR,<sup>(10)</sup> and IGF-1R.<sup>(12)</sup> Resistance to alectinib is reported to develop as a result of mechanisms such as EGFR ligands, *MET* gene amplification,<sup>(25)</sup> overexpression of IGF-1R and the activation of *MET* via HGF.<sup>(15,26)</sup> Thus, the activation of EGFR may be a common route by which numerous types of cancer acquire the resistance to targeted therapy. Sustained

EGFR activity can be caused by ligand stimulation as well as *EGFR* mutations. In the present study, while the crizotinib-resistant #2 cells did not have any common *EGFR* mutations (exon 19 deletion or L858R) or the T790M mutation, they did produce a high level of EGFR ligand (AREG), activate EGFR, and thereby cause crizotinib resistance. Since #2 cells with high AREG expression showed cross-resistance to alectinib and ceritinib, AREG must be considered along with other EGFR ligands as common factors for resistance to ALK inhibitors.

Epidermal growth factor receptor ligands are not only produced by cancer cells, but also by stromal cells such as fibroblasts, macrophages, and vascular endothelial cells. We previously reported that exposing *EML4-ALK*-positive lung cancer cells to EGFR ligands (EGF, HB-EGF, and TGF- $\alpha$ ) in a paracrine manner triggers ALK-TKI resistance.<sup>(26)</sup> In contrast, crizotinib-resistant cell lines established in an *in vivo* model produced AREG and developed resistance in an autocrine manner (Fig. 3a). While mechanism by which AREG expression was upregulated in these cells is unknown at present, previous studies reported that the expression of the AREG was induced by activating the AMP/PKA pathway via prostaglandin E<sub>2</sub>,<sup>(27)</sup> cigarette smoke,<sup>(28)</sup> hypoxia,<sup>(29)</sup> or by stimulation with inflammatory cytokines such as IL-1 and TNF $\alpha$ .<sup>(30)</sup> Further studies are warranted to clarify underlying mechanisms.

The pro-AREG protein that is expressed on the cell membrane after transcription and translation is cleaved after stimulation with inflammatory cytokines such as IL-1 $\beta$ ,<sup>(31)</sup> IL-8,<sup>(32)</sup> and TNF $\alpha$ ,<sup>(33)</sup> that protein is secreted as AREG. Secreted AREG activates signaling via EGFR, which in turn produces autostimulatory feedback that activates the transcription of AREG. Thus, inflammatory cytokines play an important role in the expression of AREG. We established a crizotinib-resistant cell line from pleural effusion of mice with carcinomatous pleurisy where various cytokine may exist. Inflammatory cytokines in pleural effusion potentially led to an increased AREG level in cancer cells. Unexpectedly, expression of other EGFR ligands was not increased, or in fact decreased, in #2 cells in comparison to the A925L parent cell line. Tani *et al.*<sup>(17)</sup> indicated that TGF- $\alpha$  levels increased in an alectinib-resistant cell line that was established *in vitro*. This disparity is assumed to be due to the cell line and drugs used, as well as

differences in the conditions under which resistance was induced (*in vitro* versus *in vivo*).

Interestingly, the level of phosphorylated ALK in #2 cells was also lower than that in the parental cells. Therefore, it is possible that #2 cells were less dependent on ALK signaling for survival than the parental cells, though #2 cells still showed a low degree of sensitivity to crizotinib. In this unique situation, the survival signals from phosphorylated EGFR may confer crizotinib resistance in #2 cells, even though the level of phosphorylated EGFR in #2 cells was lower than that in the parental A925LPE3 cells. To clarify the underlying mechanisms by which low levels of phosphorylated EGFR were sufficient to induce crizotinib resistance in #2 cells, it is necessary to perform additional studies in the future.

Future topics include how to detect resistance as a result of EGFR bypass signaling in patients. Kim *et al.*<sup>(34)</sup> reported that patients with crizotinib-resistant *ALK*-rearranged lung cancer have elevated levels of AREG in their pleural effusions. Therefore, in addition to the identification of gene mutations (*ALK*, *EGFR*, *KRAS*, etc.) that confer drug resistance in cancer cells in fluids, measurement of various ligands (including AREG) in the fluids may be crucial in cases where resistance developed as a result of cancer in the fluids (e.g. pleural effusion, ascites, and pericardial effusion).

In conclusion, we produced SCID mouse model of carcinomatous pleurisy with *EML4-ALK* lung cancer cells and induced acquired resistance to crizotinib by continuous oral treatment with crizotinib. We further established crizotinib resistant cells and found that amphiregulin (AREG), an EGFR ligand, is largely responsible for the activation of EGFR in an autocrine manner and in turn leads to resistance to crizotinib. Moreover, we demonstrated that crizotinib resistance could be overcome by inhibiting EGFR bypass signaling *in vivo*. Therefore, inhibition of EGFR signaling may be a promising strategy to overcome crizotinib resistance in *EML4-ALK* lung cancer.

## Disclosure Statement

Seiji Yano obtained research grants from Chugai Pharma, and Boehringer-Ingelheim, and honoraria from Chugai Pharma and Boehringer-Ingelheim. The other authors have no conflict of interest. This work was supported by JSPS KAKENHI Grant Numbers JP16H05308 (to SY).

## References

- Soda M, Choi YL, Enomoto M *et al.* Identification of the transforming *EML4-ALK* fusion gene in non-small-cell lung cancer. *Nature* 2007; **448**: 561–6.
- Camidge DR, Doebele RC. Treating ALK-positive lung cancer—early successes and future challenges. *Nat Rev Clin Oncol* 2012; **9**: 268–77.
- Shaw AT, Yeap BY, Mino-Kenudson M *et al.* Clinical features and outcome of patients with non-small-cell lung cancer who harbor *EML4-ALK*. *J Clin Oncol* 2009; **27**: 4247–53.
- Camidge DR, Bang YJ, Kwak EL *et al.* Activity and safety of crizotinib in patients with ALK-positive non-small-cell lung cancer: updated results from a phase I study. *Lancet Oncol* 2012; **13**: 1011–9.
- Shaw AT, Kim DW, Nakagawa K *et al.* Crizotinib versus chemotherapy in advanced ALK-positive lung cancer. *N Engl J Med* 2013; **368**: 2385–94.
- Solomon BJ, Mok T, Kim DW *et al.* First-line crizotinib versus chemotherapy in ALK-positive lung cancer. *N Engl J Med* 2014; **371**: 2167–77.
- Doebele RC, Pilling AB, Aisner DL *et al.* Mechanisms of resistance to crizotinib in patients with ALK gene rearranged non-small cell lung cancer. *Clin Cancer Res* 2012; **18**: 1472–82.
- Katayama R, Shaw AT, Khan TM *et al.* Mechanisms of acquired crizotinib resistance in ALK-rearranged lung cancers. *Sci Transl Med* 2012; **4**: 120ra117.
- Choi YL, Soda M, Yamashita Y *et al.* *EML4-ALK* mutations in lung cancer that confer resistance to ALK inhibitors. *N Engl J Med* 2010; **363**: 1734–9.
- Sasaki T, Koivunen J, Ogino A *et al.* A novel ALK secondary mutation and EGFR signaling cause resistance to ALK kinase inhibitors. *Cancer Res* 2011; **71**: 6051–60.
- Katayama R, Khan TM, Benes C *et al.* Therapeutic strategies to overcome crizotinib resistance in non-small cell lung cancers harboring the fusion oncogene *EML4-ALK*. *Proc Natl Acad Sci USA* 2011; **108**: 7535–40.
- Lovly CM, McDonald NT, Chen H *et al.* Rationale for co-targeting IGF-1R and ALK in ALK fusion-positive lung cancer. *Nat Med* 2014; **20**: 1027–34.
- Sakamoto H, Tsukaguchi T, Hiroshima S *et al.* CH5424802, a selective ALK inhibitor capable of blocking the resistant gatekeeper mutant. *Cancer Cell* 2011; **19**: 679–90.
- Ou SH, Ahn JS, De Petris L *et al.* Alectinib in crizotinib-refractory ALK-rearranged non-small-cell lung cancer: a phase II global study. *J Clin Oncol* 2016; **34**: 661–8.

- 15 Isozaki H, Ichihara E, Takigawa N *et al.* Non-small cell lung cancer cells acquire resistance to the ALK inhibitor alectinib by activating alternative receptor tyrosine kinases. *Cancer Res* 2016; **76**: 1506–16.
- 16 Katayama R, Friboulet L, Koike S *et al.* Two novel ALK mutations mediate acquired resistance to the next-generation ALK inhibitor alectinib. *Clin Cancer Res* 2014; **20**: 5686–96.
- 17 Tani T, Yasuda H, Hamamoto J *et al.* Activation of EGFR bypass signaling by TGF $\alpha$  overexpression induces acquired resistance to alectinib in ALK-translocated lung cancer cells. *Mol Cancer Ther* 2016; **15**: 162–71.
- 18 Nanjo S, Nakagawa T, Takeuchi S *et al.* *In vivo* imaging models of bone and brain metastases and pleural carcinomatosis with a novel human EML4-ALK lung cancer cell line. *Cancer Sci* 2015; **106**: 244–52.
- 19 Green LM, Reade JL, Ware CF. Rapid colorimetric assay for cell viability: application to the quantitation of cytotoxic and growth inhibitory lymphokines. *J Immunol Methods* 1984; **70**: 257–268.
- 20 Nakataki E, Yano S, Matsumori Y *et al.* Novel orthotopic implantation model of human malignant pleural mesothelioma (EHMES-10 cells) highly expressing vascular endothelial growth factor and its receptor. *Cancer Sci* 2006; **97**: 183–91.
- 21 Gainor JF, Dardaei L, Yoda S *et al.* Molecular mechanisms of resistance to first- and second-generation ALK inhibitors in ALK-rearranged lung cancer. *Cancer Discov* 2016 Oct; **6**: 1118–1133.
- 22 Suda K, Tomizawa K, Fujii M *et al.* Epithelial to mesenchymal transition in an epidermal growth factor receptor-mutant lung cancer cell line with acquired resistance to erlotinib. *J Thorac Oncol* 2011; **6**: 1152–61.
- 23 Yamaguchi N, Lucena-Araujo AR, Nakayama S *et al.* Dual ALK and EGFR inhibition targets a mechanism of acquired resistance to the tyrosine kinase inhibitor crizotinib in ALK rearranged lung cancer. *Lung Cancer* 2014; **83**: 37–43.
- 24 Singh B, Carpenter G, Coffey RJ. EGF receptor ligands: recent advances. *F1000Res* 2016; **5**: (F1000 Faculty Rev):2270.
- 25 Toyogawa G, Seto T, Takenoyama M, Ichinose Y. Crizotinib can overcome acquired resistance to CH5424802: is amplification of the MET gene a key factor? *J Thorac Oncol* 2014; **9**: e27–8.
- 26 Tanimoto A, Yamada T, Nanjo S *et al.* Receptor ligand-triggered resistance to alectinib and its circumvention by Hsp90 inhibition in EML4-ALK lung cancer cells. *Oncotarget* 2014; **5**: 4920–8.
- 27 Shao J, Lee SB, Guo H, Evers BM, Sheng H. Prostaglandin E2 stimulates the growth of colon cancer cells via induction of amphiregulin. *Cancer Res* 2003; **63**: 5218–23.
- 28 Du B, Altorki NK, Kopelovich L, Subbaramaiah K, Dannenberg AJ. Tobacco smoke stimulates the transcription of amphiregulin in human oral epithelial cells: evidence of a cyclic AMP-responsive element binding protein-dependent mechanism. *Cancer Res* 2005; **65**: 5982–8.
- 29 O'Reilly SM, Leonard MO, Kieran N *et al.* Hypoxia induces epithelial amphiregulin gene expression in a CREB-dependent manner. *Am J Physiol Cell Physiol* 2006; **290**: C592–600.
- 30 Woodworth CD, McMullin E, Iglesias M, Plowman GD. Interleukin 1 alpha and tumor necrosis factor alpha stimulate autocrine amphiregulin expression and proliferation of human papillomavirus-immortalized and carcinoma-derived cervical epithelial cells. *Proc Natl Acad Sci USA* 1995; **92**: 2840–4.
- 31 Liu FL, Wu CC, Chang DM. TACE-dependent amphiregulin release is induced by IL-1beta and promotes cell invasion in fibroblast-like synoviocytes in rheumatoid arthritis. *Rheumatology (Oxford)* 2014; **53**: 260–9.
- 32 Tanida S, Joh T, Itoh K *et al.* The mechanism of cleavage of EGFR ligands induced by inflammatory cytokines in gastric cancer cells. *Gastroenterology* 2004; **127**: 559–69.
- 33 Berasain C, Nicou A, Garcia-Irigoyen O *et al.* Epidermal growth factor receptor signaling in hepatocellular carcinoma: inflammatory activation and a new intracellular regulatory mechanism. *Dig Dis* 2012; **30**: 524–31.
- 34 Kim S, Kim TM, Kim DW *et al.* Heterogeneity of genetic changes associated with acquired crizotinib resistance in ALK-rearranged lung cancer. *J Thorac Oncol* 2013; **8**: 415–22.

## Supporting Information

Additional Supporting Information may be found online in the supporting information tab for this article:

**Fig. S1.** Crizotinib is equally effective against A925L and A925LPE3 cells.

**Fig. S2.** Morphological changes in each cell line.

**Fig. S3.** Crizotinib with either erlotinib or cetuximab is not sufficiently effective for APE-CR.

**Fig. S4.** The combined use of crizotinib and erlotinib or cetuximab led the higher expression of cleaved PARP than crizotinib alone.

**Fig. S5.** High concentration of AREG induced resistance of A925LPE3 cells to crizotinib.

**Fig. S6.** Body weight of mice and representative images of tumor-bearing mice.

**DOC. S1.** The siRNA target sequences.